Songklanakarin J. Sci. Technol.
44 (3), 892–898, May – Jun. 2022

http://www.sjst.psu.ac.th

Original Article

Effect of V-cut on the performance of a longitudinal vortex generator using CFD

Ishu Shukla, Yatish Kumar Baghel, and Vivek Kumar Patel*

Department of Applied Mechanics, Motilal Nehru National Institute of Technology Allahabad, Prayagraj, 211004 India

Received: 29 July 2021; Revised: 31 December 2021; Accepted: 3 March 2022

Abstract

Computational analysis is conduct to investigate the comparative study between V-cut vortex generator and without V-cut vortex generator at different spacing lengths. Water is the working fluid, and the Reynolds number is varying in the range of 300 to 1,500. Computational results are validated with the available literature, and SST k-ω turbulence model is used for the computational analysis. The performances of both designs are compared by using performance evaluation criteria (PEC). Friction factor, heat transfer rate, and performance evaluation criteria are evaluated in both cases for different spacing ratio (2-8) between the vortex generators. The overall performance evaluation criterion for the modified design (V-cut vortex generator) is found to increase in the range of 0.66 to 6.18% as compared to the original design (without V-cut vortex generator). They concluded that the modified design is more effective as compared to the original design.

Keywords: friction factor, PEC, turbulence modelling, V-cut vortex generator

1. Introduction

The use of turbulator enhances the heat transfer rate by disrupting the thermal boundary layer. Passive turbulators do not require any external power source and they are more economical. In the passive techniques, the use of inserts is highly cost effective as it is easy to install and uninstall as per the heat enhancement requirement. Manglik and Bergles (1993) performed the experiment to study the heat transfer rate and established mathematical relations for twisted tape inserts in a tube under constant wall temperature condition for both transient and turbulent flow. Eiamsa-ard, Thianpong, and Promvonge (2006) performed an experimental study on the discontinuous twisted tape elements and found that with increasing twist ratio heat transfer get enhanced and friction factor was comparatively less for spaced twisted tape. Peng *et al.*, (2007) did an experimental study on shell and tube heat exchanger with continuous helical baffles and they found that the rate of heat transfer increased by 10% as compared to segmented baffles. Ahmadvand, Najafi, and Shahidinejad (2010) performed both experimental and computational analysis on heat transfer and flow attributes of decaying swirl generated in the pipe directed by the axial vanes. Similarly, Eiamsa-ard and Promvonge (2010) studied the effect of propeller type swirl generator on convective heat transfer in the round tube. They found that heat transfer increases both with increasing number of vanes and the blade angle as well. Solano, García, Vicente, and Viedma (2011) performed an experimental investigation on tubes of heat exchangers with motionless scraper and they observed that this technique was even better than twisted tape in the laminar regime as it reduced the fouling as well. Duangthongsuk and Wongwises (2013) studied the different types of turbine type swirl generators installed in a tube and its effects on the augmentation of heat transfer through experimentally. Nanan, Thianpong, Promvonge, and Eiamsa-Ard (2014) analyzed the heat transfer enhancement by using the perforated helical twisted tape through experimentally. Pal and Saha (2015) conducted an experimental study on spiral corrugated tube along with the twisted tape installed and they observed that the frictional losses is 63-107% and 182% increase in heat transfer rate. Wen, Yang, Wang, Xue, and Tong (2015) performed a numerical investigation on ladder baffles installed in a heat exchanger which solved the problem of

*Corresponding author
Email address: vivek@mnnit.ac.in

triangular leakage zones in case of helical baffles. Rate of heat transfer and friction factor both increased after the installation of swirl vanes in the shell and tube heat exchanger by Yehia, Attia, Abdelatif, and Khalil (2016). Gorman, Sparrow, Ilamparuthi, and Minkowycz (2016) studied on swirl generated by a fan and its effect on heat transfer in a turbulent pipe flow. Heat transfer rate was enhanced by cylindrical blade installed in a tube by Karagoz, Afshari, Yildirim, and Comakli (2017). An experimental and numerical study performed by Liu, Zheng, Shan, Liu, and Liu (2018) on a circular tube equipped with multiple conical strips inserts generated longitudinal vortices which increased the rate of heat transfer as well as friction factor. Bhattacharyya, Benim, Chattopadhyay, and Banerjee (2019) performed an experiment on corrugated tube having spring tape which increased the convective heat transfer in the turbulent regime. A new technique involving novel ball- type turbulator is used by Afshari, Zavaragh, and Di Nicola (2019) which increases heat transfer rate through vortex generation. Finned tube heat exchanger is another solution provided by Awais and Bhuiyan (2019) to increase the heat transfer rate with minimum pressure drop. Ibrahim, Essa, and Mostafa (2019) performed a computational investigation on heat transfer improvement in circular tube inserted with conical rings. They found an appreciable increase in Nusselt number from 330- 765% by using different converging diverging arrangements of the ring. Nakhchi and Esfahani (2019) increased the performance of twisted tape by providing a double V- cut which in return would generate an extra vortex helping achieve high rate of heat transfer. Baghel and Patel (2020) conducted the experiment as well as computational analysis to study the heat transfer enhancement through the air jet impingement on a flat plate. The effect of impingement height of a circular jet with nanofluids on the heat transfer rate was studied by Pratap, Baghel, and Patel (2020) and they observed the increase in heat transfer by using the nanofluids. Alimoradi, Fatahi, Rehman, Khoshvaght-Aliabadi, and Hassani (2020) studied the effects of twisted tabulators at uniform wall heat flux condition on both rate of heat transfer and the frictional losses. In the given literature, the use of conventional inserts achieved the goal of heat transfer enhancement while paying the cost in terms of extreme pressure drop. The extreme pressure drop further leads to increase in pumping power consumption. Therefore, this work presented here focuses on the issue of heat transfer enhancement along with minimal pressure drop. This goal can be achieved with the help of longitudinal vortex generator which has been designed with the help of four equally spaced conical slices attached to the rod at optimum spacing length. By providing a V-cut to the conical slices the pressure drop can be reduced further.

In this study, a small V-cut of 0.5 mm is carved in the original design of the insert having a 70° central angle for varying the spacing ratio (S/D) from 2 to 8. The effect of this V-cut on the heat transfer rate and pressure drop is analyzed in terms of Nusselt number (Nu) and friction factor (f), respectively. The performance evaluation criteria is also calculated in order to analyze the efficiency of the modified design as compared to the original design.

2. Materials and Methods

2.1 Geometry and grid generation

Solid Works software is used to design the vortex generator (or insert), and Figure 1 shows the geometry of the V-cut vortex generator. Insert consists of a conical slice that has been cut from the truncated cone having a fixed cone angle $\theta = 40^{o}$ having a thickness of 3 mm. The central line of the cone and rod intersect at an angle of $\theta/2$. This conical slice has been connected to a 3 mm long connecting rod at the truncated end through which it has been attached to the central rod of 2 mm diameter. An additional feature, known as slice height (H) has been introduced (H = 8 mm) along with constant slant angle (α) = 40º in order to generate a scouring effect near the pipe wall region and helps in determining the cone-diameter. The set of four slices are attached to the central rod at varying spacing ratio (S/D = 2 - 8), and the central angle is 70º in order to study its effect on heat transfer rate. These four slices will generate a set of 4 longitudinal vortexes, and this longitudinal vortex is creating turbulence in the flow field. The length (L) of the insert used in the computational setup is 550 mm, having 50 mm downstream length, and is inserted in the pipe of diameter (D) 20 mm having negligible wall thickness as shown in Figure 2. Further, a small V-notch of 0.5 mm depth is carved in the conical slices of the insert having 70° central angle for varying length spacing ratio. The size of the V-cut on the vortex generator has been optimized in such a way that the heat transfer enhancement due to scouring effect does not gets hampered completely and the maximum overall heat transfer rate can be obtained while minimizing the pressure drop appreciably. If the depth of the V-cut is increased then the initial concavity provided to the longitudinal vortex generator becomes insignificant. As the vortex generator will not be able to direct the flow towards the wall and the scouring effect will get permanently hampered. Meanwhile, if we keep the depth of V-cut less than 0.5 mm the strength of small vortex produced will not be enough to enhance the heat transfer rate. Therefore, the depth of the V-cut has been optimized at 0.5 mm.

An unstructured tetrahedron grid is generated of the computational flow domain as shown in Figure 3. The grid independence test (GIT) is performed on the circular tube having an insert of 70˚ central angle, slant height of 8 mm, and 40 mm length spacing at Re = 300 by varying the number of elements from 2,276,004 to 6,659,742 in order to determine the optimum grid size. The variation of Nu is not changing frequently beyond this grid size 5,205,200. Therefore, this grid size 5,205,200 is used for further investigations.

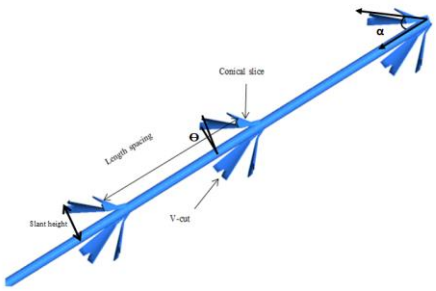

Figure 1. V-cut vortex generator

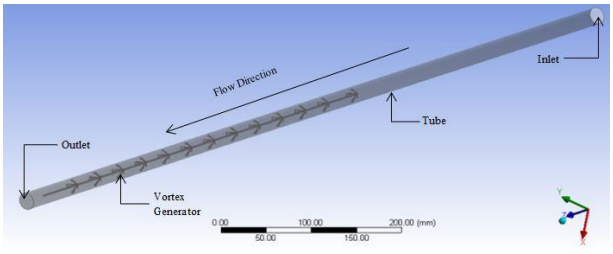

Figure 2. Computational flow domain

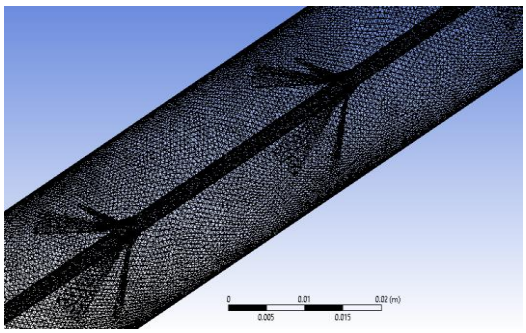

Figure 3. Grid generation of the flow domain

2.2 Governing equations and turbulence modeling

The working fluid is water, and it is assumed to be incompressible, isotropic, continuous, and has constant physical property irrespective of temperature. Equations (1- 3) are representing the governing equations that are used in the present study (Fluent 2011).

Continuity equation

$$\frac{\partial \rho}{\partial t} + \frac{\partial}{\partial x_i}(\rho U_i) = 0 \quad (1)$$

Momentum equation

$$\frac{\partial}{\partial t}(\rho U_i) + \frac{\partial}{\partial x_i}(\rho u_i u_j) = -\frac{\partial P}{\partial x_i} + \frac{\partial \tau_{ij}}{\partial x_j} \quad (2)$$

Energy equation

$$\frac{\partial}{\partial t}(\rho h_{xx}) + \frac{\partial}{\partial x_j}(\rho h_{xx} U_j) = \frac{\partial P}{\partial t} + \frac{\partial}{\partial x_j}(u_i \tau_{ij} + \gamma \frac{\partial T}{\partial x_j}) \quad (3)$$

In order to capture the vortex flow, turbulence modeling is adopted. Therefore, SST k-ω model is used in the present work. Transport equations for SST k- ω model are given as Fluent (2011) and Dewan (2010).

$$\frac{\partial(\rho k)}{\partial t} + \frac{\partial(\rho k u_i)}{\partial x_i} = \frac{\partial}{\partial x_i}\left(\tau_k \frac{\partial k}{\partial x_j}\right) + G_K - Y_k + S_k \quad (4)$$

$$\frac{\partial(\rho \omega)}{\partial t} + \frac{\partial(\rho \omega u_i)}{\partial x_i} = \frac{\partial}{\partial x_j}\left(\tau_\omega \frac{\partial \omega}{\partial x_j}\right) + G_\omega - Y_\omega + D_\omega + S_\omega \quad (5)$$

2.3 Mathematical formulation

Reynolds number (Re) for both enhanced tube and smooth tube without an insert is calculated by Equation 6. In contrast, the local heat transfer coefficient (h) and average Nusselt number (Nu_z) about the circumference are given by equations (7) and (8). Equation 9 is used to calculate the friction factor across the tube. The equivalent Reynolds number (Re_e) is calculated by the equation (10). Equations (6 - 9) are taken from Holman (2002) and Gnielinski (1976).

$$Re = \rho U_m D/\mu \quad (6)$$

$$h(z,\varphi) = q/(T_w(z,\varphi) - T_m) \quad (7)$$

$$Nu_z(avg.) = \frac{\oint Nu(z,\emptyset)\, d\emptyset}{\oint d\emptyset} \quad (8)$$

$$f = \frac{\Delta P}{\left(\frac{L}{D}\right)\rho U^2/2} \quad (9)$$

$$(Re_a)^3 f_a = (Re_e)^3 f_e \quad (10)$$

The efficiency of the modified design is compared to the original design with the help of performance evaluation criteria. Desmukh and Vedula (2014) provide the detail of the Equations (10 – 11).

$$PEC = \frac{\frac{Nu}{Nue}}{\left(\frac{f}{fe}\right)^{\frac{1}{3}}} \quad (11)$$

2.4 Boundary conditions and solution methods

Boundary conditions are provided in the form of fully developed flow at inlet thus, providing uniform velocity and temperature profile. Equation (12) and (13) are representing the velocity and temperature profile equations (Holman 2002 and Gnielinski 1976). The outflow condition is applied at outlet. Constant heat flux condition 2,000 W/m^2 is assessed on the external surface of the tube and the Reynolds number is varied from 300 to 1,500.

$$U = U_c\left(1 - \frac{r^2}{R^2}\right) \quad (12)$$

$$T = T_c + \frac{qR}{\gamma}\left[\left(\frac{r}{R}\right)^2 - \frac{1}{4}\left(\frac{r}{R}\right)^4\right] \quad (13)$$

All the equations are solved in commercial software ANSYS FLUENT. Figure 4 represents the flow chart of the adopted methodology. SIMPLE algorithm is used for pressure-velocity coupling and 2nd order upwind scheme is used for discretization. The convergence criteria for both continuity and momentum equation are set at 10^{-4} and for energy equation it's kept at 10^{-6}.

3. Results and Discussion

3.1 Validation of the CFD results

First, the computational results of the simple tube are validated with the experimental results of the simple tube (Deshmukh *et al.*, 2016) in terms of both Nusselt number and friction factor within an average error of 0.16% and 3.6% respectively as shown in Figure 5. In the present work,

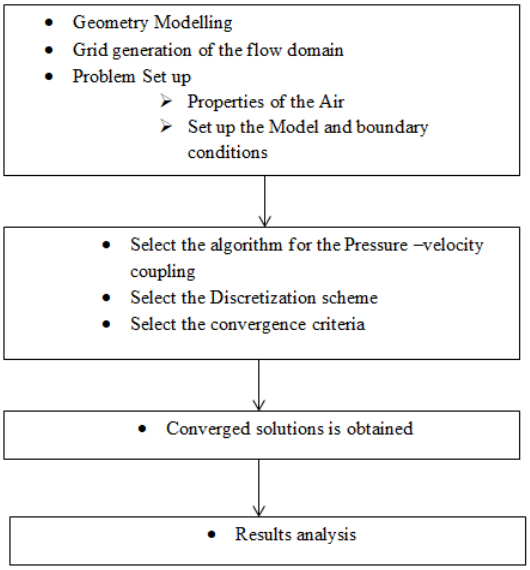

Figure 4. Flow chart of the adopted methodology

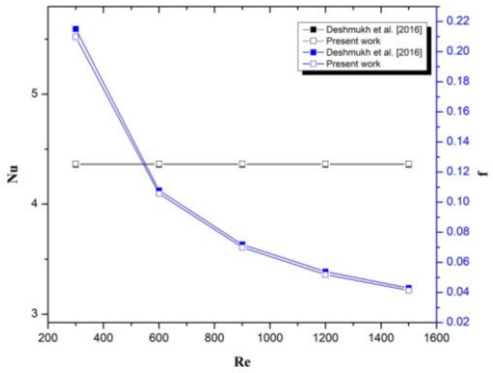

Figure 5. Validation of plain tube

computational results are validated with the experimental results of Deshmukh, Prabhu, and Vedula (2016) as shown in Figure 6. The ratio of with insert and without the insert in terms of Nusselt number and friction factor are calculated for the validation. Figure 6 shows that the computational results are in good agreement with the Deshmukh *et al.*, (2016), and 10.79% error in Nusselt number and 7.89% error in friction factor are observed as compared to the experimental results. SST k-ω turbulence model is used for the simulation, and it is also observed that the SST k-ω turbulence model is used for further simulations.

3.2 Effects on the friction factor and Nusselt number

The flow of water in the axial direction inside the circular tube was restricted by the originally designed insert. The fluid flow restriction in the pipe is reduced by providing a specific space by carving a V-cut in an originally designed insert. In the original design, the conical slices of the vortex generator give the direction of the water flow towards the wall and disrupt the thermal boundary layer. After the formation of the V-cut in the original design, the flow of water is divided

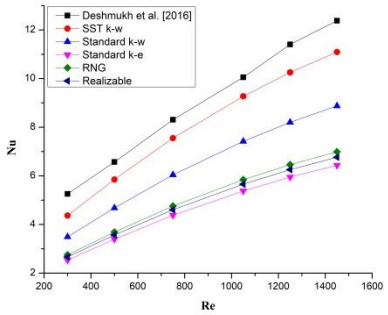

(a)

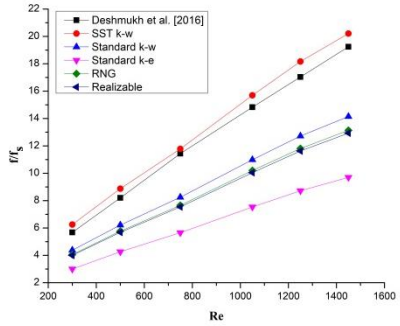

(b)

Figure 6. Validation of present study with Deshmukh *et al.* (2016)

into two parts. One part of the water flow is used to generate a small vortex near the V-cut and while the rest of the part of the flow is unrestricted in the axial direction of the pipe. Figure 7 shows the variation of the ratio of friction factor at different Reynolds numbers for several of spacing ratio. The friction factor ratio increases with the increase in Reynolds number and decreases with the increase in length spacing. Compared to the original design, the friction factor value on average has been reduced by 32.59%. Hence, the pressure drop is reduced in the case of V-cut provided in the slice of the original design as compared to without a V-cut.

Vortexes are generated near each slice, as shown in the Figure 8. Hence, the heat transfer rate is increased due to the generation of vortexes. Conical slice (without V-cut) is providing the direction of the flow of water towards the wall. Therefore, the thermal boundary layer is disturbed near the wall, and this phenomenon is known as the scouring effect. After disrupting the boundary layer, the flow of water impinged back in the core region between the two conical slices. This impingement of flow is responsible for further enhancing the rate of heat transfer near the central region. Additional vortexes are generated near the V-cut, as shown in the Figure 9, but the strength of impingement of water is decreased as compared to conical slice (without V-notch) in the central region. Therefore, the effect of scouring gets is low, and the overall heat transfer rate is decreased. Hence, the rate of heat transfer is reduced as compared to the original design (without V-notch). Figure 9 represents the variation of the velocity and temperature distribution in the transverse plane along the tube for S/D = 2. The fully developed velocity and temperature profile change significantly and become more uniform from inlet to outlet.

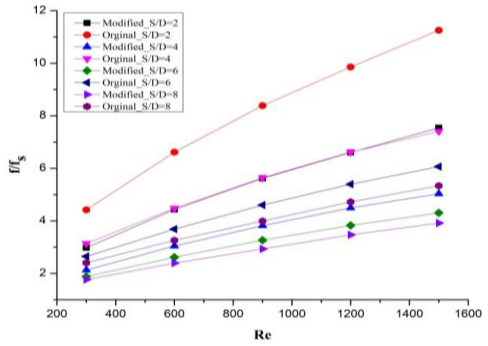

Figure 7. Variation of f/f_s for modified and original design for different S/D ratio

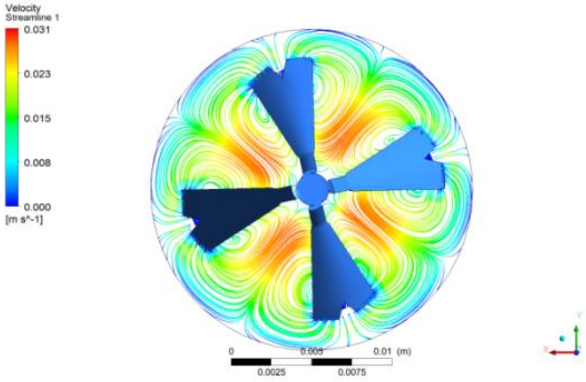

Figure 8. Streamline near the slice and V-cut

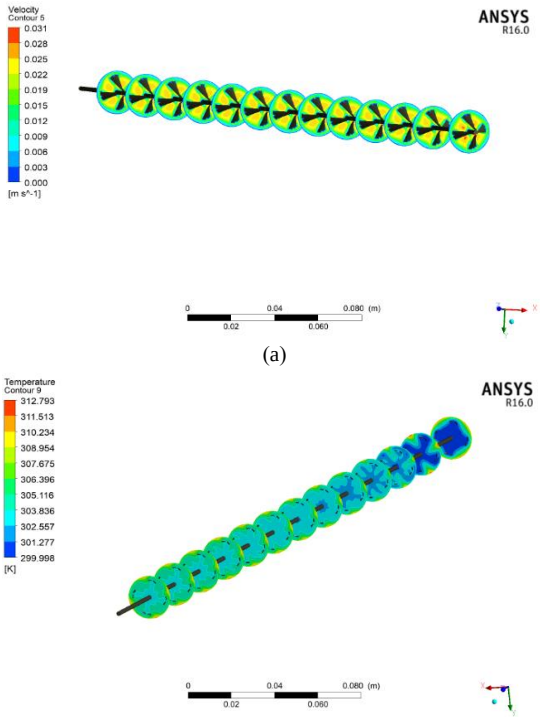

Figure 9. Flow structure for S/D = 2: (a) velocity distribution, (b) temperature distribution

Figure 10 shows the variation of the Nusselt number along the vortex generator for the various S/D ratio. The average Nusselt number increases with the increase in S/D ratio. As water flow through the vortex generators, the average Nusselt number increases proportionally for all S/D ratio. Figure 11 shows the variation of Nusselt number of the modified design and original design for different spacing ratio at various Reynolds numbers. It is also clearly observed that the ratio of Nu is decreasing with the increase in spacing length as shown in the figure 11. The overall performance evaluation criteria is the efficient method to know the effectiveness of the modified design (V-cut in vortex generator). PEC provides the mutual evaluation for both hydraulic and thermal performances at constant pumping power. Figure 12 show the comparison of PEC between original and modified design at different spacing ratio. It is observed that the PEC for modified design at different spacing length is greater than the original design in a range of 0.66% to 6.18%. Hence, a modified design is more effective as compared to the original design.

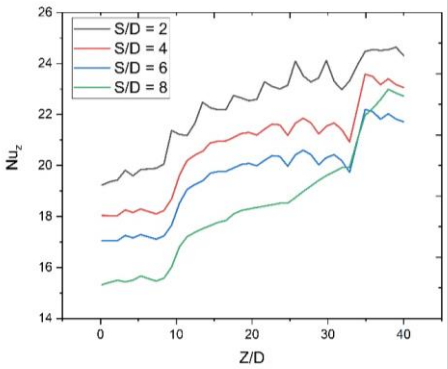

Figure 10. Nusselt number along the vortex generator for various S/D ratio

4. Conclusions

In this investigation, the comparative study between the V-cut vortex generator and without V- cut vortex generator in terms of friction factor, heat transfer rate, and the effectiveness for different spacing lengths in the horizontal pipe has been performed. The SST k-ω model is in good agreement with the experimental data. 10.79% error in Nu and 7.89% error in friction factor (f) are observed as compared to the experimental results (Deshmukh *et al.*, 2016). The ratio of Nusselt number increases with the increase in Reynolds number and decreases with the increase in length spacing. The heat transfer rate in the form of Nusselt number reduces by 19.5% compared to the original design due to the loss of scouring effect. The friction factor ratio increases with the increase in Reynolds number and decreases with the increase in length spacing. In the V-cut vortex generator, 32.59% friction factor is reduced as compared to the without V-cut vortex generator. The overall performance evaluation criterion for the modified design (V-cut vortex generator) increases in the range of 0.66 to 6.18% as compared to the original design (without V-cut vortex generator). Hence, the modified design is more effective as compared to the original design.

Nomenclature

f	Friction factor of Circular Tube with insert
f_e	Equivalent friction factor for smooth circular tube
f_s	Friction factor of the smooth tube
Nu	Nusselt number for circular tube with insert
Nu_e	Equivalent Nusselt Number for smooth tube
Nu_s	Nusselt Number for smooth tube
Re_a	Reynolds number for augmented case
Re_e	Equivalent Reynolds Number for the smooth pipe
T	Temperature of water (K)
T_c	Temperature of water at the tube centre (K)
T_m	Water Bulk mean temperature (K)
T_w	Local temperature of the tube wall (K)
u	Velocity of water (m/s)
U_i	Velocity of water in 3 dimensional flow (m/s)
U_c	Velocity of water at the tube centre (m/s)
U_m	Mean velocity of water (m/s)
γ	Thermal conductivity of water (W/m K)
ρ	Density of water (Kg/m^3)
Nu_a	Average Nusselt Number for with insert
τ_{ij}	Three dimensional normal Shear stress (N/m^2)
h_{xx}	Local convective heat transfer coefficient in x-direction (W/m^{2}K)
μ	Dynamic Viscosity of water (Kg/m-s)
G_k	Generation of Turbulent kinetic energy due to mean velocity gradient
G_ω	Generation of ω
τ_k	Effective diffusivity of k
τ_ω	Effective diffusivity of ω
Y_k	Dissipation of k due to turbulence
Y_ω	Dissipation of ω due to dissipation
D_ω	Cross diffusion term
S_k	Source function for k
S_ω	Source function for ω
S	Space length (m)
D	Diameter of the tube (m)
Θ	Central angle (degree)
α	Slant angle (degree)

References

Afshari, F., Zavaragh, H. G., & Di Nicola, G. (2019). Numerical analysis of ball-type turbulators in tube heat exchangers with computational fluid dynamic simulations. *International Journal of Environmental Science and Technology*, *16*(7), 3771-3780.

Ahmadvand, M., Najafi, A. F., & Shahidinejad, S. (2010). An experimental study and CFD analysis towards heat transfer and fluid flow characteristics of decaying swirl pipe flow generated by axial vanes. *Meccanica*, *45*(1), 111-129.

Alimoradi, A., Fatahi, M., Rehman, S., Khoshvaght-Aliabadi, M., & Hassani, S. M. (2020). Effects of transversely twisted-turbulators on heat transfer and pressure drop of a channel with uniform wall heat flux. *Chemical Engineering and Processing-Process Intensification*, *154*, 108027.

Awais, M., & Bhuiyan, A. A. (2019). Enhancement of thermal and hydraulic performance of compact finned-tube heat exchanger using vortex generators (VGs): a parametric study. *International Journal of Thermal Sciences*, *140*, 154-166.

Baghel, Y. K., & Patel, V. K. (2020). Experimental and computational analysis of heat transfer by a turbulent air jet impingement on a flat surface. *Advances in Mechanical Engineering*, 85-96.

Bhattacharyya, S., Benim, A. C., Chattopadhyay, H., & Banerjee, A. (2019). Experimental investigation of heat transfer performance of corrugated tube with spring tape inserts. *Experimental Heat Transfer*, *32*(5), 411-425.

Deshmukh, P. W., & Vedula, R. P. (2014). Heat transfer and friction factor characteristics of turbulent flow through a circular tube fitted with vortex generator inserts. *International Journal of Heat and Mass Transfer*, *79*, 551-560.

Deshmukh, P. W., Prabhu, S. V., & Vedula, R. P. (2016). Heat transfer enhancement for laminar flow in tubes using curved delta wing vortex generator inserts. *Applied Thermal Engineering*, *106*, 1415-1426.

Dewan, A. (2010). *Tackling turbulent flows in engineering*. Berlin, Germany: Springer Science and Business Media.

Duangthongsuk, W., & Wongwises, S. (2013). An experimental investigation of the heat transfer and pressure drop characteristics of a circular tube fitted with rotating turbine-type swirl generators. *Experimental Thermal and Fluid Science*, *45*, 8-15.

Eiamsa-ard, S., & Promvonge, P. (2010). Thermal characterization of turbulent tube flows over diamond-shaped elements in tandem. *International Journal of Thermal Sciences*, *49*(6), 1051-1062.

Eiamsa-ard, S., Thianpong, C., & Promvonge, P. (2006). Experimental investigation of heat transfer and flow friction in a circular tube fitted with regularly spaced twisted tape elements. *International Communications in Heat and Mass Transfer*, *33*(10), 1225-1233.

Fluent, A. N. S. Y. S. (2011). Fluent 14.0 user's guide. *ANSYS FLUENT Inc*.

Gnielinski, V. (1976). New equations for heat and mass transfer in turbulent pipe and channel flow. *International Journal of Chemical Engineering*, *16*(2), 359-368.

Gorman, J. M., Sparrow, E. M., Ilamparuthi, S., & Minkowycz, W. J. (2016). Effect of fan-generated swirl on turbulent heat transfer and fluid flow in a pipe. *International Journal of Heat and Mass Transfer*, *95*, 1019-1025.

Holman J. P. (2002). *Heat transfer: Instructor's solutions manual to accompany*. New York, NY: McGraw-Hill.

Ibrahim, M. M., Essa, M. A., & Mostafa, N. H. (2019). A computational study of heat transfer analysis for a circular tube with conical ring turbulators. *International Journal of Thermal Sciences*, *137*, 138-160.

Karagoz, S., Afshari, F., Yildirim, O., & Comakli, O. (2017). Experimental and numerical investigation of the cylindrical blade tube inserts effect on the heat transfer enhancement in the horizontal pipe exchangers. *Heat and Mass Transfer*, *53*(9), 2769-2784.

Liu, P., Zheng, N., Shan, F., Liu, Z., & Liu, W. (2018). An experimental and numerical study on the laminar heat transfer and flow characteristics of a circular tube fitted with multiple conical strips inserts. *International Journal of Heat and Mass Transfer*, *117*, 691-709.

Manglik, R. M., & Bergles, A. E. (1993). Heat transfer and pressure drop correlations for twisted-tape inserts in isothermal tubes: Part II—Transition and turbulent flows. *Journal of Heat Transfer*, *115*(4), 890-896.

Nakhchi, M. E., & Esfahani, J. A. (2019). Performance intensification of turbulent flow through heat exchanger tube using double V-cut twisted tape inserts. *Chemical Engineering and Processing-Process Intensification*, *141*, 107533.

Nanan, K., Thianpong, C., Promvonge, P., & Eiamsa-Ard, S. (2014). Investigation of heat transfer enhancement by perforated helical twisted-tapes. *International Communications in Heat and Mass Transfer*, *52*, 106-112.

Pal, S., & Saha, S. K. (2015). Laminar fluid flow and heat transfer through a circular tube having spiral ribs and twisted tapes. *Experimental Thermal and Fluid Science*, *60*, 173-181.

Peng, B., Wang, Q. W., Zhang, C., Xie, G. N., Luo, L. Q., Chen, Q. Y., & Zeng, M. (2007). An experimental study of shell-and-tube heat exchangers with continuous helical baffles. *Journal of Heat Transfer*, *129*(10), 1425-1431

Pratap, A., Baghel, Y. K., & Patel, V. K. (2020). Effect of impingement height on the enhancement of heat transfer with circular confined jet impingement using nanofluids. *Materials Today: Proceedings*, *28*, 1656-1661.

Solano, J. P., García, A., Vicente, P. G., & Viedma, A. (2011). Flow field and heat transfer investigation in tubes of heat exchangers with motionless scrapers. *Applied Thermal Engineering*, *31*(11-12), 2013-2024.

Wen, J., Yang, H., Wang, S., Xue, Y., & Tong, X. (2015). Experimental investigation on performance comparison for shell-and-tube heat exchangers with different baffles. *International Journal of Heat and Mass Transfer*, *84*, 990-997.

Yehia, M. G., Attia, A. A., Abdelatif, O. E., & Khalil, E. E. (2016). Heat transfer and friction characteristics of shell and tube heat exchanger with multi inserted swirl vanes. *Applied Thermal Engineering*, *102*, 1481-1491.